

## Evaluation of the distribution of subtropical free tropospheric humidity in AMIP-2 simulations using METEOSAT water vapor channel data

H. Brogniez, R. Roca, and L. Picon

Laboratoire de Météorologie Dynamique, CNRS/IPSL, Palaiseau, France

Received 9 August 2005; revised 23 August 2005; accepted 12 September 2005; published 8 October 2005.

[1] In the framework of the Atmospheric Model Intercomparison Project (AMIP) phase 2, we have established a diagnostic of the free tropospheric humidity (FTH) distribution using METEOSAT data over the 1984–1995 period for 14 climate models. The methodology of evaluation follows a two step “model-to-satellite” approach. First the raw METEOSAT “Water Vapor” radiances are simulated from the model profiles of temperature and humidity using the RTTOV-7 radiative transfer model. Second, the radiances are converted into FTH using the same coefficients as in the satellite product offering a direct comparison. The analysis is focused on the dry subtropical areas observed by METEOSAT: the Eastern Mediterranean and the tropical South Atlantic Ocean. Most of the models reproduce the observed seasonal cycle both in terms of phasing and magnitude, despite an overall moist bias. A few models are in close agreement with the satellite data. The magnitude of the satellite estimated inter-annual variability is also generally captured by models. Again, a small subset of models shows close agreement with the observations. This comparison suggests general improvements of the models with respect to the AMIP-1 simulations. **Citation:** Brogniez, H., R. Roca, and L. Picon (2005), Evaluation of the distribution of subtropical free tropospheric humidity in AMIP-2 simulations using METEOSAT water vapor channel data, *Geophys. Res. Lett.*, 32, L19708, doi:10.1029/2005GL024341.

### 1. Introduction

[2] Water vapor is a major greenhouse gas and is usually considered to play an amplifying role in global warming through a strongly positive climate feedback loop [e.g., Ramanathan, 1981; Held and Soden, 2000]. Due to non linearity in the radiative transfer, outgoing longwave radiation (OLR) is more sensitive to small humidity perturbations in a dry environment than in a moist region. For instance, increasing the free tropospheric humidity (FTH) from 5% to 10% and keeping temperature constant, decreases OLR by  $10 \text{ Wm}^{-2}$  while increasing FTH from 25% to 30% only modifies OLR by less than  $5 \text{ Wm}^{-2}$  [Spencer and Braswell, 1997]. This confers a central role to the dry subtropical free troposphere regions in the radiation budget and its sensitivity [Pierrehumbert, 1995]. Humidity in the mid-to-upper troposphere (500–200 hPa) is usually estimated thanks to infrared radiometers centered on the 6.3 microns water vapor absorption band, which are avail-

able on operational satellite platforms. This is commonly known as Upper Tropospheric relative Humidity. Over the dry regions of the intertropical belt, these radiometers are sensitive to a broader layer of the atmosphere, typically ranging from 700–100 hPa and well suited for investigating our key regions. We will hence refer to these satellite measurements as Free Tropospheric Humidity (FTH) [Roca *et al.*, 2003; Brogniez *et al.*, 2004]. The adequate representation of these large radiative sinks in the current generation of general circulation models (GCMs) is an important step towards realistic climate simulations and climate sensitivity estimation. Using various water vapor related satellite observational datasets and methods, a number of studies have provided evaluation of the intertropical tropospheric humidity distribution of GCMs [e.g., Soden and Bretherton, 1994; Chen *et al.*, 1996; Roca *et al.*, 1997; Bates and Jackson, 1997; Allan *et al.*, 2003] highlighting a wide range of model behavior. Here, we present a direct and dedicated comparison between satellite observations of tropospheric humidity and GCMs simulations. The comparisons are furthermore performed systematically for 14 models participating in the AMIP-2 (Atmospheric Model Intercomparison Project) project using a novel METEOSAT dataset covering the subtropical Atlantic Ocean and African continent over the 1984–1995 period. The focus of the analysis is on the seasonal cycle and on the inter-annual variability of dry subtropical areas using a consistent model-to-satellite approach for all the models. First the data and the methodology of the comparison are introduced. The results are then presented and their relevance to previous intercomparisons is discussed.

### 2. Data and Method

[3] The approach for the comparison follows the model-to-satellite technique. The GCMs outputs are used to simulate synthetic radiances similar to the satellite observations using the RTTOV-7 radiative code [Matricardi *et al.*, 2004]. Then both observed and simulated radiances are converted into a geophysical humidity parameter to help interpreting the differences between models and observations. The observed reference consists of the 6.3microns METEOSAT “Water Vapor” (WV) channel data inverted in terms of layer-mean relative humidity following the technique introduced by Soden and Bretherton [1993]. The actual width of the layer depends upon the temperature and humidity profile as well as the observing geometry. In the dry subtropical regions of interest here, this layer spans the whole free troposphere. The FTH algorithm and climatology are detailed by Roca *et al.* [2003], Brogniez *et al.*

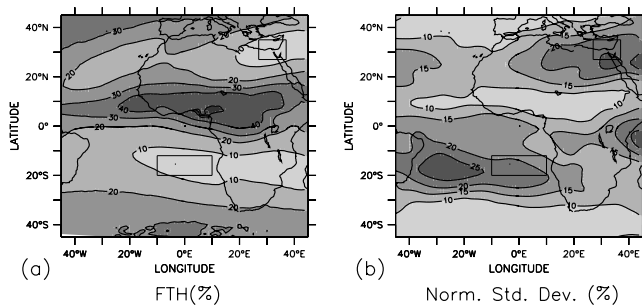


**Figure 1.** Boreal summer June–July–August 1984–1995. (a) Multi-year mean of FTH in % and (b) normalized standard deviation in %. The rectangles show the two regions of interest.

[2004], Brogniez [2004] and here, we only report its most salient features. The algorithm follows Soden and Bretherton's approach, but, for the computation, substitutes their climatological temperature profile by the actual temperature profiles from ERA40. Also, in order to define the contributing layer, the Jacobian of the brightness temperature (BT) with respect to relative humidity was selected among other weighting functions. A careful selection of the scenes is performed following Schmetz and Turpeinen [1988] using the cloud top pressure data from the ISCCP-DX dataset [Rossow and Schiffer, 1999]. This selection conserves scenes with low levels clouds, which do not influence the BT, thus yielding to an enhanced sampling of the oceanic subtropical areas. The FTH climatology is constructed using the homogeneous BTs archive developed at LMD [Picon et al., 2003] from the ISCCP-B3 raw data and spans the 1983–1995 period with a 3 hourly resolution.

[4] The final product uncertainty can be decomposed into retrieval and calibration uncertainties. This algorithm results in a negligible bias and to an absolute RMS error of 1.59% over a large ensemble of training profiles, in good agreement with other techniques [e.g., Bates and Jackson, 2001]. In terms of relative errors, the present algorithm is characterized by a RMS smaller than 10% over a wide range of humidity conditions from very dry to almost saturated including a 0.5K ( $\sim 5\%$ ) uncertainty due to the radiative transfer code [Matricardi et al., 2004]. Note that the use of the same retrieval for both observations and models minimizes the algorithm-based bias in the comparison. Concerning the calibration of the dataset, the coefficients have been adjusted to take into account the recently highlighted warm bias of 2–3 K of the METEOSAT WV channel [e.g., Köpken et al., 2003] following Bréon et al. [2000], using spatially and temporally collocated HIRS-12/NOAA-12 data. This best estimate of the calibration bias lies within 5–10% (0.5–1 K) which translates into  $\sim 10\%$  relative uncertainty in FTH [e.g., Van de Berg et al., 1995; Bréon et al., 2000]. However, it does not impact much the evaluation of models, which is mainly based on comparisons of variances.

[5] Figure 1a shows the multi-year average of FTH for the boreal summer season June–July–August. The moist ITCZ separates the two dry zones of large scale subsidence, one in each hemisphere. Two very dry regions with values of FTH below 10% are observed over the Eastern Mediterranean Sea (Region 1: 27E–37E/27N–35N) and over the

Southern tropical Atlantic Ocean (Region 2: 10W–10E/12S–20S) close to the St Helen highs. Region 1 is further characterized by a large inter-annual standard deviation normalized with respect to the mean ( $\sigma_N = 23\%$ , Figure 1b) and is located in a larger homogeneous area. Region 2 covers a less homogeneous area and exhibits a more complex spatial structure of interannual variability. Although only covering a small part of the Earth's surface, these two regions are representative of the distribution and variability of FTH over a larger domain corresponding to the whole Atlantic/Africa subtropical subsidence regimes [Brogniez et al., 2002] and will then be used to evaluate the GCMs performance.

[6] The Atmospheric Model Intercomparison Project (AMIP) [Gates et al., 1999] is an international effort to generate comparable integrations from many atmospheric general circulation models and to provide systematic evaluations of these integrations. A number of so-called diagnostics are then performed onto these simulations spanning a wide range of variables, processes and scales. Here, we report on the diagnostic #34 dedicated to free tropospheric humidity [Roca and Picon, 1999]. At the time of writing, required outputs were available for 14 models presented in Table 1. Monthly means of specific humidity and temperature profiles over the 1984–1995 period from each of the GCMs are used to compute synthetic METEOSAT BTs using a model-to-satellite approach: BTs are first computed with the RTTOV-7 radiative code from the humidity and temperature fields, and are then converted into FTH using the algorithm developed for the observations, hence minimizing the methodological bias [see Soden and Bretherton, 1994; Roca et al., 1997]. The use of monthly mean profiles to compute the BTs for comparison to the satellite observations was driven by the data availability within the project; it will therefore not account for the intra-seasonal variability of FTH in models. While over

**Table 1.** Statistics of the 14 AMIP-2 Evaluated Models for Boreal Summer June–July–August<sup>a</sup>

Model #	Model Name Institution	Interannual Mean, in % RH		Interannual Normalized Standard Deviation, %	
		Region1	Region 2	Region 1	Region 2
0	METEOSAT	7.3	8.5	23.7	19.7
1	CCCMA	<b>9.6</b>	<b>8.6</b>	<b>25</b>	<b>22.1</b>
2	CCSR	<b>7.9</b>	<b>10.2</b>	<b>22.8</b>	<b>19.6</b>
3	CNRM	22.6	23.2	24.8	21.1
4	ECMWF	16.4	14.1	18.9	18.4
5	JMA	11.6	14.6	<b>17.2</b>	<b>17.1</b>
6	MGO	18.4	16.7	<b>8.7</b>	5.4
7	MPI	14.9	15.2	18.8	14.5
8	NCAR	19.7	16.7	25.9	22.2
9	NCEP	18.1	11.5	25.4	<b>19.1</b>
10	PNNL	14.5	28.5	22.8	14.7
11	SUNYA	21.0	16.3	26.2	30.1
12	UGAMP	<b>9.2</b>	<b>10.6</b>	<b>22.8</b>	<b>22.6</b>
13	UIUC	16.0	37.4	<b>16.3</b>	10.2
14	UKMO	13.7	5.6	21.2	12.5

<sup>a</sup>See <http://www.pcmdi.llnl.gov/amip> for the acronyms and models institutions list as well as the details of their formulation. The satellite estimations are also provided. Shown are the 10% (bold) and 1% (italic) significance level for means and variances tests (Student's t-test for the mean and Fisher-Snedecor test for the variance). Note that tests computations are performed on the absolute values although normalized values are listed.

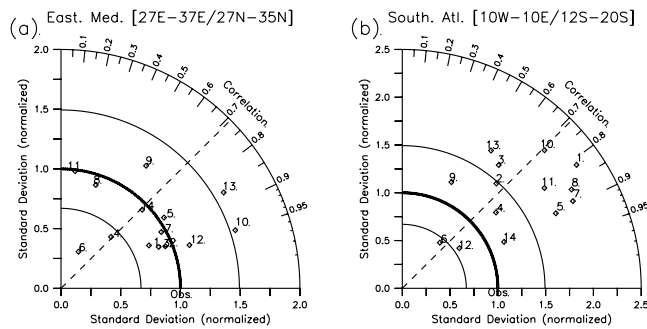


**Figure 2.** Taylor diagrams describing the 1984–1995 averaged seasonal cycle of FTH over the two regions. Each number represents one of 14 models listed in Table 1. The radius line shows the correlation t-test significance value at the 1% level. The two circles delineate the variance test (Fisher-Snedecor) at the 10% level. Computations are performed using the absolute values and the models variances are normalized to the observations for easy viewing.

the deep tropics this might bias the comparisons with the satellite, over the dry subtropical areas of interest here such methodological bias is small [Chen *et al.*, 1996; Roca and Picon, 1999], compared to the differences between observations and models that are reported below. For instance, the monthly mean of FTH for July 1992 constructed using ERA40 6 hourly temperature and humidity profiles differs from the mean FTH obtained from the monthly mean profiles by less than 1.5% over the two regions of interest.

### 3. Results

[7] The FTH maps from individual models (not shown) indicate that most of the models indeed exhibit relative minima in the Regions 1 and 2 and that the reported differences are not due to shifts in the spatial structures and are therefore representative of the humidity distribution of the dry areas. The behavior of the models over the two very dry regions for the boreal summer season is summarized in Table 1. Generally, the models suffer from an absolute positive bias reaching up to 15.3% (28.9%) over the Region 1 (2). This general subtropical moist bias goes with an overall tendency for a moist bias in the tropical free troposphere of the participating models [Ross *et al.*, 2002]. Nevertheless, 4 models produce summer mean values similar to the observed one over at least one of the two considered regions. Three models (models #1, 2 and 12) reproduce the observed summer climatology over both hemispheres. The representation of the 1984–1995 multi-year averaged seasonal cycle in the models is assessed using Taylor diagrams [Taylor, 2001] which, by using correlation and normalized standard deviations, allows to overcome bias issues in the comparison. As discussed in the Introduction, non linearity in the radiative transfer suggests that small perturbations of the humidity can have an important effect on the top of the atmosphere radiation depending on the dryness of the environment. As a result, *relative* errors and variations are better related to the radiative impact of FTH than *absolute* errors are and hence will be used in the following to discuss models and observations agreement.

The observed seasonal cycle is characterized, over both regions, by a drying during summer (FTH~10%) with respect to winter (FTH~25%). The multi-year mean seasonal variance reaches 7.4% (3.2%) in absolute and 41.5% (26%) in relative values for Region 1 (2). Generally, the models perform well with the seasonal cycle and exhibit statistically significant correlation coefficients over both regions. Over the Eastern Mediterranean Sea (Figure 2a), most of the models (#1, 2, 3, 5, 7, 12 and 14) are able to reproduce magnitude and phase (at the 1% level of significance) of the observed seasonal variance of the free tropospheric humidity. Over the Southern Atlantic Ocean region (Figure 2b), correlation coefficients remain high but the models generally reveal a seasonal variance whose magnitude is significantly larger than the observed one. Nevertheless, a subset of the models agrees quantitatively with the satellite data (models #4, 12 and 14). In summary, at the seasonal scale, and despite a general moist bias, models appear to reproduce the observed variability, and a small group of models actually performs in very close agreement with the observations over the two dry subtropical area diagnosed here.

[8] At the inter-annual scale, the FTH distribution over the dry regions is characterized by normalized variances of around 25% of the signal (equivalent to 2–3 K in terms of BT). The magnitude of the maximum variation encountered over Region 1 almost reaches 50% relative, the driest summer being 1984 (FTH~4%) and the least dry 1992 (FTH~7%). None of the evaluated models either correlates significantly with the observations over this period or simulates the sequence of these extreme summer conditions. Nevertheless, as presented in Table 1, the models tend to reproduce inter-annual variances similar to the satellite estimate over one or the other region. A few models perform equally well over both the Mediterranean and Atlantic Ocean regions (models # 1, 2, 5 and 12) with simulated inter-annual variance similar to the observations using a 10% confidence interval.

### 4. Discussion

[9] The present diagnostic study consists in comparing in a systematic and methodologically consistent way the distribution of FTH over two dry subtropical regions, simulated by 14 GCMs participating in AMIP-2, to the climatology derived from METEOSAT observations. Whereas no such diagnostics were performed as part of AMIP-1 (the first phase of AMIP), a similar type of comparisons proposed by Bates and Jackson [1997] reveals a substantial increase in the quality of the representation of some of the features of the FTH distribution. For many AMIP-2 models, the major gain concerns the closer agreement to the satellite archive at the seasonal scale compared to the model participating in AMIP-1, although many models still suffer from significant bias (mainly moist bias) over the subtropical areas. At the inter-annual scale, significant departures from the observations dominate the results of the intercomparison which seems to be confirmed by other tropical diagnostics [e.g., Srinivasan, 2003; Weare, 2004] although the magnitude of the inter-annual signal is often consistent with the satellite estimations. An important outcome of the present effort is that a small subset of the participating models indeed shows a very close agreement

with the observations over the different scales investigated here. Like with many other results of AMIP diagnostics, the present study nevertheless does not permit to connect any bias or type of model answers to any special resolution choice or to any parameterized physics selection [see also Ross *et al.*, 2002]. For instance, model #2 is spectral and is run on a T21 grid ( $\sim 5.6^\circ \times 5.6^\circ$ ) with 18 vertical levels, and uses a mass flux convective scheme, whereas model #12 is a grid point model ran at a  $2.5^\circ \times 3.75^\circ$  resolution over 58 vertical levels with a moist adjustment convection scheme, and both models nevertheless perform equally well with respect to the observations. Due to a lack of availability of models outputs at short time scales, the intra-seasonal and synoptic time scales could not be investigated, but the results presented here show that a few models perform well enough to qualify for more detailed investigations. The subtropical free tropospheric humidity is indeed driven by large scale dynamics at synoptic scales [e.g., *Pierrehumbert and Roca*, 1998; *Waugh*, 2005] and systematic evaluation of the intra-seasonal variability of FTH in the GCMs in connection to their dynamics could give some insight in the processes at play in the models and thus a more physically based understanding of the reasons for their better representation of the seasonal mean distribution reported here. The METEOSAT database appears particularly well suited for such investigations down to daily time scales.

## References

- Allan, R., M. Ringer, and A. Slingo (2003), Evaluation of moisture in the Hadley Centre climate model using simulations of HIRS water-vapor channel radiances, *Q. J. R. Meteorol. Soc.*, **129**, 3371–3389.
- Bates, J., and D. Jackson (1997), A comparison of water vapor observations with AMIP-1 simulations, *J. Geophys. Res.*, **102**, 21,837–21,852.
- Bates, J., and D. Jackson (2001), Trends in upper-tropospheric humidity, *Geophys. Res. Lett.*, **28**, 1695–1698.
- Bréon, F.-M., D. Jackson, and J. Bates (2000), Calibration of the METEOSAT water vapor channel using collocated NOAA/HIRS-12 measurements, *J. Geophys. Res.*, **105**, 11,925–11,933.
- Brogniez, H. (2004), Humidité de la troposphère libre africaine: Elaboration d'une archive Meteosat, analyse climatique et evaluation de modèles, Ph.D. thesis, Univ. Pierre et Marie Curie, Paris.
- Brogniez, H., R. Roca, and L. Picon (2002), First results of the AMIP2 GCMs evaluation using METEOSAT water vapor data, *Proceedings of the AMIP Workshop: Towards Innovative Model Diagnostics*, report, World Clim. Res. Program, Toulouse, France, 12–15 Nov. (Available at <http://www-pcmdi.llnl.gov/projects/amip>)
- Brogniez, H., R. Roca, and L. Picon (2004), Interannual and intraseasonal variabilities of the free tropospheric humidity using METEOSAT water vapor channel over the tropics, paper presented at EUMETSAT Meteorological Satellite Conference, Prague 31 May–4 June.
- Chen, C.-T., E. Roeckner, and B. Soden (1996), A comparison of satellite observations and model simulations of column-integrated moisture and upper-tropospheric humidity, *J. Clim.*, **9**, 1561–1585.
- Gates, W., et al. (1999), An overview of the results of the Atmospheric Model Intercomparison Project (AMIP-I), *Bull. Am. Meteorol. Soc.*, **80**, 29–55.
- Held, I., and B. Soden (2000), Water vapor feedback and global warming, *Annu. Rev. Energy Environ.*, **25**, 441–475.
- Köpken, C., J.-N. Thépaut, and G. Kelly (2003), Assimilation of geostationary WV radiances from GOES and METEOSAT at ECMWF, *Res. Rep. 14*, EUMETSAT/ECMWF Fellowship Program, Reading, U. K.
- Matricardi, M., F. Chevallier, G. Kelly, and J.-N. Thépaut (2004), An improved general fast radiative transfer model for the assimilation of radiance observations, *Q. J. R. Meteorol. Soc.*, **130**, 153–173.
- Picon, L., R. Roca, S. Serrar, and M. Desbois (2003), A new METEOSAT “water vapor” archive for climate studies, *J. Geophys. Res.*, **108**(D10), 4301, doi:10.1029/2002JD002640.
- Pierrehumbert, R. T. (1995), Thermostats, radiator fins and the local runaway greenhouse, *J. Atmos. Sci.*, **52**, 1784–1806.
- Pierrehumbert, R. T., and R. Roca (1998), Evidence for control of Atlantic subtropical humidity by large scale advection, *Geophys. Res. Lett.*, **25**, 4537–4540.
- Ramanathan, V. (1981), The role of ocean-atmosphere interactions in the CO<sub>2</sub>-climate problem, *J. Atmos. Sci.*, **38**, 918–930.
- Roca, R., and L. Picon (1999), Evaluation of convection and upper-level moisture and their links using Meteosat water vapor channel and GCM results, *AMIP-2 Diagn. Subproj.*, **34**.
- Roca, R., L. Picon, M. Desbois, H. Le Treut, and J.-J. Morcrette (1997), Direct comparison between METEOSAT water vapor channel and GCM results, *Geophys. Res. Lett.*, **24**, 147–150.
- Roca, R., H. Brogniez, L. Picon, and M. Desbois (2003), Free tropospheric humidity observations from METEOSAT water vapor data, J3.7, paper presented at 83rd Annual Meeting, Am. Meteorol. Soc., Long Beach, Calif., 9–13 Feb.
- Ross, R., W. Elliott, and D. Seidel (2002), Lower-tropospheric temperature-humidity relationships in radiosonde observations and Atmospheric General Circulation Models, *J. Hydrometeorol.*, **3**, 26–38.
- Rossov, W., and R. Schiffer (1999), Advances in understanding clouds from ISCCP, *Bull. Am. Meteorol. Soc.*, **80**, 2269–2287.
- Schmetz, J., and O. Turpeinen (1988), Estimation of the upper tropospheric relative humidity field from METEOSAT water vapor image data, *J. Appl. Meteorol.*, **27**, 889–899.
- Soden, B., and F. Bretherton (1993), Upper tropospheric relative humidity from the GOES 6.7  $\mu\text{m}$  channel: Method and climatology for July 1987, *J. Geophys. Res.*, **98**, 16,669–16,688.
- Soden, B., and F. Bretherton (1994), Evaluation of water vapor distribution in general circulation models using satellite observations, *J. Geophys. Res.*, **99**, 1187–1210.
- Spencer, R., and W. Braswell (1997), How dry is the tropical free troposphere? Implications for a global warming theory, *Bull. Am. Meteorol. Soc.*, **78**, 1097–1106.
- Srinivasan, J. (2003), Diagnostic study of errors in the simulation of tropical continental precipitation in general circulation models, *Ann. Geophys.*, **21**, 1197–1207.
- Taylor, K. (2001), Summarizing multiple aspects of model performance in a single diagram, *J. Geophys. Res.*, **106**, 7183–7192.
- Van de Berg, L., J. Schmetz, and J. Whitlock (1995), On the calibration of the METEOSAT water vapor channel, *J. Geophys. Res.*, **100**, 21,069–21,076.
- Waugh, D. W. (2005), Impact of potential vorticity intrusions on subtropical upper tropospheric humidity, *J. Geophys. Res.*, **110**, D11305, doi:10.1029/2004JD005664.
- Weare, B. (2004), A comparison of AMIP II model cloud layer properties with ISCCP D2 estimates, *Clim. Dyn.*, **22**, 281–292.

H. Brogniez, L. Picon, and R. Roca, Laboratoire de Météorologie Dynamique, CNRS/IPSL, F-91128 Palaiseau, France. (roca@lmd.polytechnique.fr)